International Journal of Pharmaceutics 392 (2010) 170–177

Contents lists available at ScienceDirect

International Journal of Pharmaceutics

journal homepage: www.elsevier.com/locate/ijpharm

Design and evaluation of micellar nanocarriers for 17-allyamino-17-demethoxygeldanamycin (17-AAG)

Thripthy Chandran[a,1], Usha Katragadda[a,1], Quincy Teng[b], Chalet Tan[a,*]

[a] Department of Pharmaceutical Sciences, College of Pharmacy and Health Sciences, Mercer University, 3001 Mercer University Drive, Atlanta, GA 30341, United States
[b] National Exposure Research Laboratory, Environmental Protection Agency, 960 College Station Road, Athens, GA 30605, United States

ARTICLE INFO

Article history:
Received 15 January 2010
Received in revised form 21 March 2010
Accepted 27 March 2010
Available online 2 April 2010

Keywords:
Polymeric micelles
PEG-DSPE
TPGS
17-AAG
Drug release

ABSTRACT

17-Allyamino-17-demethoxygeldanamycin (17-AAG) is a potent anticancer agent currently undergoing phases I and II clinical trials. However, the clinical development of 17-AAG has been hindered by its poor aqueous solubility and hepatotoxicity. This study aimed to devise novel micellar nanocarriers for 17-AAG that improve its solubility and retain the incorporated drug for a prolonged period of time. We have found that 1,2-distearoyl-*sn*-glycero-3-phosphoethanolamine-*N*-[methoxy(polyethylene glycol)-2000]/D-α-tocopheryl polyethylene glycol 1000 (PEG-DSPE/TPGS) mixed micelles (at a 1:2 molar ratio) can deliver 17-AAG at clinically relevant doses. By modulating the concentrations of micelle-forming copolymers, the burst release of 17-AAG from PEG-DSPE/TPGS mixed micelles was substantially reduced with a release half-life up to about 8 h. Our ^{1}H NMR spectroscopy results revealed that the incorporation of TPGS into PEG-DSPE micelles restricted internal molecular motions of copolymers in both the corona and core regions of the micelles, leading to the delayed drug release. Cytotoxicity of 17-AAG formulated in PEG-DSPE/TPGS mixed micelles against human ovarian cancer SKOV-3 cells was comparable to that of free 17-AAG. 17-AAG-loaded PEG-DSPE/TPGS mixed micelles may offer a promising alternative to the current 17-AAG formulations for the treatment of solid tumors.

1. Introduction

Heat shock protein 90 (Hsp90) is a highly conserved intracellular chaperon protein that is responsible for conformational maturation and stability of a myriad of signaling proteins, including HER2, BCR-ABL, estrogen receptors, androgen receptors, insulin-like growth factor 1 receptor, hypoxia-inducible factor 1α, B-Raf, cdk4 and Akt among numerous others (Whitesell and Lindquist, 2005). Geldanamycin and its anaologs are able to compete with ATP at the nucleotide binding site on the N-terminal domain of Hsp90 and inhibit its essential ATPase activity, leading to the degradation of its client proteins by the ubiquitin–proteasome pathway (Isaacs et al., 2003). Because many of these oncogenic client proteins are involved in hallmark traits of malignancy, such as deregulated cell cycle progression, anti-apoptosis, angiogenesis, invasion and metastasis, inhibition of Hsp90 confers a potent combinatorial blockade on the cancer phenotype.

17-Allylamino-17-demethoxygeldanamycin (17-AAG) is the first Hsp90 inhibitor entering clinical trials in patients with advanced cancers including metastatic prostate, melanoma, lung, colon, pancreatic, head and neck, ovarian and breast cancers (Goetz et al., 2005; Grem et al., 2005; Solit et al., 2007; Weigel et al., 2007; Heath et al., 2008; Solit et al., 2008). Based on the promising preclinical results, 17-AAG is also being tested clinically in combination with other targeted treatments or conventional chemotherapy (Ramalingan et al., 2008; Tse et al., 2008; Modi et al., 2007). Due to its poor aqueous solubility (~10 μg/ml, 17 μM) and low oral bioavailability, 17-AAG is formulated in intravenous solutions that require 4% DMSO or 20% Cremophor EL as organic excipients. DMSO causes serious side effects such as nausea, vomiting and malodor, and is known to be potentially hepatotoxic and cardiotoxic. Cremophor EL induces hypersensitivity reactions that necessitate the pretreatment with antihistamines and corticosteroids. Moreover, 17-AAG causes serious hepatotoxicity, which is attributable to extensive distribution and metabolism of the drug in the liver (Egorin et al., 2001; Guo et al., 2008). Owing to these toxicities associated with the currently available formulations, 17-AAG is administered to patients no more frequently than twice a week. Thus far, few objective responses have been observed in patients receiving the single or combination therapy, suggesting that the higher and/or more sustained concentration of 17-AAG in the tumor is required to exert adequate Hsp90 inhibition. An improved formulation for 17-AAG is therefore urgently needed to eliminate the use of toxic organic excipients as well as to allow for better drug delivery to the tumor tissue with alleviated hepatotoxicity.

* Corresponding author. Tel.: +1 678 547 6240; fax: +1 678 547 6423.
E-mail address: tan_c@mercer.edu (C. Tan).
[1] These authors contributed equally to the work.

0378-5173/$ – see front matter © 2010 Elsevier B.V. All rights reserved.
doi:10.1016/j.ijpharm.2010.03.056

IPI-504, a highly soluble hydroquinone hydrochloride derivative of 17-AAG, is currently under clinical development (Erlichman, 2009). However, due to its sensitivity to the oxidizing environment and rapid interconversion with 17-AAG in cells and *in vivo* (Sydor et al., 2006), IPI-504 is likely to share the clinical toxicities of 17-AAG. 17-Dimethylaminoethylamino-17-demethoxygeldanamycin (17-DMAG) is a second-generation geldanamycin derivative now in phase I testing. 17-DMAG is administered orally owing to its higher aqueous solubility and greater oral bioavailability than 17-AAG (Egorin et al., 2002). Despite these apparent improvements, preclinical studies have shown that the hepatotoxicity of 17-DMAG is dose-limiting, and the maximum tolerated dose of 17-DMAG is significantly lower than 17-AAG, suggesting intermittent treatment breaks or weekly dosing will still be required (Glaze et al., 2005; Hollingshead et al., 2005).

Biocompatible and biodegradable polymeric micelles (10–100 nm in diameter) are recognized as one of the most promising nanovectors for poorly water-soluble drugs. Several cytotoxic anticancer drugs (e.g. doxorubicin, paclitaxel and cisplatin) formulated in such nanovectors are presently in clinical trials with encouraging results (Nishiyama and Kataoka, 2006; Matsumura, 2008). Self-assembled from amphiphilic copolymers, polymeric micelles can solubilize hydrophobic drugs by incorporating the drug molecules in the vicinity of the hydrophobic core, and remain intact upon dilution in a large volume of blood (Gaucher et al., 2005). Restricted from the normal vasculature (1–2 nm fenestrations in most healthy tissues), long-circulating nanovectors can extravasate and accumulate at the tumor site via the enhanced permeability and retention (EPR) effect, owing to the leaky vasculature (usually >100 nm fenestrations) and the impaired lymphatic drainage in solid tumors (Matsumura and Maeda, 1986). The conjugates of polyethylene glycol (PEG) and diacyllipids, such as PEG-distearoylphosphatidylethanolamine (PEG-DSPE), form stable micelles in aqueous environment because of strong hydrophobic interaction between double acyl chains of phospholipid residues (Gao et al., 2002). PEG-DSPE micelles are spheroidal and have a narrow size distribution of 7–35 nm, depending on the molecular size (750–5000 Da) of the PEG block. With a critical micelle concentration (CMC) in 10^{-6} to 10^{-5} M range, PEG-DSPE micelles retain their size even after 48-h incubation in plasma (Lukyanov et al., 2002). A number of sparingly water-soluble anticancer drugs, such as paclitaxel, tamoxifen and doxorubicin, can be incorporated into PEG-DSPE micelles (Gao et al., 2002; Musacchio et al., 2009; Tang et al., 2007). The small and uniform particle size of PEG-DSPE micelles offers a distinct advantage in terms of targeted drug delivery to the tumor tissue via the EPR effect. The administration of doxorubicin-loaded PEG-DSPE micelles lead to extensive drug accumulation and penetration in the tumor, greatly enhancing the anticancer efficacy of the drug in tumor-bearing mice (Tang et al., 2007).

In the present work, we report on the design of PEG-DSPE micellar nanocarriers for 17-AAG without the inclusion of any organic solvent. We found that by modulating the PEG-DSPE concentration and incorporating D-α-tocopheryl polyethylene glycol 1000 succinate (TPGS) in the micelle composition, the burst release of 17-AAG from the micelles was significantly reduced. These PEG-DSPE/TPGS mixed micelles have the potential to be further functionalized to achieve active targeting of 17-AAG to tumor cells.

2. Materials and methods

2.1. Chemicals

1,2-Distearoyl-*sn*-glycero-3-phosphoethanolamine-*N*-[methoxy(polyethylene glycol)-2000] (ammonium salt, PEG-DSPE) was purchased from Avanti Polar Lipids, Inc. (Alabaster, AL) and used without further purification. D-α-Tocopheryl polyethylene glycol 1000 succinate (TPGS) was a gift from Eastman Co. (Kingsport, TN). 17-AAG was purchased from LC Laboratories (Woburn, MA). All other chemical reagents used were of analytical or reagent grade.

2.2. Preparation of 17-AAG-incorporating micelles

Drug-loaded micelles were prepared by a dry film method (Musacchio et al., 2009). Briefly, varying amounts of PEG-DSPE, TPGS and 17-AAG were dissolved in chloroform in a round-bottom flask. Chloroform was removed under vacuum, resulting in the formation of a homogenous film. The drug-polymer film was hydrated in 10 mM HEPES-buffered saline (pH 7.4, HBS), and sonicated at the room temperature for 10 min. The resulting mixture was centrifuged at 12,000 × *g* for 10 min to yield clear micelle dispersion.

2.3. Quantification of 17-AAG by HPLC analysis

The content of 17-AAG loaded in micelles was quantified by reverse phase HPLC based on a previously reported method (Egorin et al., 2001), which consisted of a Waters (Milford, MA) 2795 pump with an autosampler, a Waters 996 photodiode array detector and a C8 column (5 μm, i.d. 4.6 × 150 mm). The isocratic mobile phase was comprised of 75% (v/v) methanol and 25% sodium phosphate buffer (25 mM, pH 3.0) with 10 mM triethylamine at a flow rate of 1.2 ml/min. α-Naphthoflavone (Sigma, St. Louis, MO) was used as an internal standard at a concentration of 2 μM. The detection wavelength for 17-AAG and α-naphthoflavone were 333 nm and 281 nm, respectively. The standard curve of 17-AAG in phosphate buffer was linear between 0.1 μM and 10 μM. Micelle samples were diluted with the HPLC mobile phase, and injected into the HPLC system.

2.4. In vitro release of 17-AAG from micellar nanocarriers

The release of 17-AAG from micelles was evaluated by a dialysis method (Shin et al., 2009). The drug-loaded micelles were prepared with 5.3–12.5 mM PEG-DSPE, 10.6–25.0 mM TPGS and 0.6 mM 17-AAG. Post micelle preparation, each sample was diluted with HBS, a volume of 1 ml of which was loaded into a 3 ml Slide-A-Lyzer dialysis cassette (Pierce, Rockford, IL) with a MWCO of 20,000 g/mol. Each cassette was placed in 1.0 l phosphate-buffered saline (20 mM, pH 7.4), which was changed every 4 h to ensure the sink condition for the drug. A sample of 20–40 μl was drawn from each cassette at 1 h, 2 h, 4 h, 6 h, 9 h and 12 h, which was replaced by the same volume of fresh HBS. The concentration of 17-AAG in each sample was quantified by HPLC as described above.

The fraction of the drug remaining inside the dialysis cassette as a function of the release time (t) was fitted to the first-order kinetics using the following equation: $C_t/C_0 = e^{-kt}$, where C_t and C_0 are the drug concentration within the dialysis cassette at the sampling time (t) and at the initiation of the study, respectively; and k is the first-order release rate constant. The release rate constant (k) was derived from the best-fit nonlinear regression (Sigma Plot, San Jose, CA), which was used to calculate the release half-life ($t_{1/2,\ \mathrm{release}} = 0.693/k$).

2.5. Micelle size measurement

The size of the micelles was determined by dynamic light scattering using a ZETASIZER Nano-ZS (Malvern Instruments Inc., UK) equipped with He–Ne laser (4 mW, 633 nm) light source and 90° angle scattered light collection configuration. The hydrodynamic

diameter of micelles was calculated based on the Stokes–Einstein equation. All measurements were repeated three times, and data were analyzed in terms of volume-weighted particle size distribution.

2.6. Storage stability of 17-AAG-incorporating micelles

Freshly prepared 17-AAG-loaded PEG-DSPE/TPGS micelles were incubated at 37 °C for two weeks or stored at 4 °C for five weeks. At predetermined time points, the samples were centrifuged at 12,000 × *g* for 10 min, and the supernatant samples were analyzed for the changes in the particle size and drug content.

2.7. Cell proliferation assay

Human ovarian cancer SKOV-3 cells were obtained from the American Type Culture Collection (Manassas, VA) and grown in DMEM medium (Invitrogen, Carlsbad, CA) with 2 mM L-glutamine, which was supplemented with 10% (v/v) fetal bovine serum, 100 units/ml penicillin G and 100 μg/ml streptomycin. The cells were maintained at 37 °C with 5% CO_2 in a humidified incubator.

SKOV-3 cells were seeded in 96-well plates and treated in triplicate with increasing concentrations (0.025–2.5 μM) of 17-AAG either in the free form or in the micelle formulation for 72 h. Cells were fixed with 1% glutaraldehyde (Sigma), stained with 0.1% crystal violet (Sigma), and dissolved in 10% acetic acid. The plates were read at 595 nm on a spectrophotometer (Bio-Tek, Winooski, VT). The relative cell number was calculated as the percentage of the optical density of the treated sample versus that of the untreated control (Roforth and Tan, 2008).

2.8. ^1H NMR spectroscopy

Thin drug-containing lipid films were prepared as described above, and hydrated with HBS in D_2O. As controls, identical drug-containing lipid films was prepared, and then dissolved in DMSO-d_6. The concentrations of PEG-DSPE, TPGS and 17-AAG were 5.3 mM, 10.6 mM and 0.6 mM, respectively. All data were acquired on a Varian 600 MHz NMR spectrometer (Palo Alto, CA) using a 3 mm inverse probe at 20 °C, with 512 transients and 7200 Hz spectral width. For the D_2O sample, the residual water signal was suppressed using a saturation pulse with a field strength of 40 Hz. ^1H chemical shifts were referenced to internal sodium 3-(trimethylsilyl) propionate-2,2,3,3-d_4 (TSP, Sigma) at 0.0 ppm for D_2O samples and to DMSO at 2.50 ppm for DMSO-d_6 samples. The spectral full widths at half height (FWHH, $\Delta\nu_{1/2}$) were calculated using Varian VNMRJ Software (Version 2.1B).

2.9. Statistical analysis

The Student's *t*-test was used for the statistical analysis (Sigma Plot). A *p* value less than 0.05 was considered statistically significant.

3. Results

3.1. In vitro release of 17-AAG from PEG-DSPE micelles

To design an organic solvent-free formulation for 17-AAG, we attempted to incorporate 17-AAG into PEG-DSPE micelles. The drug-loaded micelles were formed efficiently, as evidenced by minimal precipitation of the starting materials. For these micelles to function as true drug carriers for 17-AAG, it is essential that the encapsulated 17-AAG molecules are retained within the micelles for an extended period of time in order to promote the drug accumulation in the tumor tissue via the EPR effect. Towards this goal, we first examined the *in vitro* release profiles of 17-AAG from PEG-DSPE micelles. The release of 17-AAG into the sink was examined by monitoring the drug concentration inside the dialysis cassette. For drug molecules to be released into the sink, they need to be first liberated from the micelles and subsequently diffuse across the dialysis membrane. To ascertain that the dialysis membrane was not a significant barrier during the release process, the release of free 17-AAG was also studied as a control. We found that, the incorporation of 17-AAG into PEG-DSPE micelles substantially reduced the release rate of 17-AAG into the sink, compared to that of free 17-AAG (Fig. 1A), indicating that the release of 17-AAG from micelles is indeed the rate-limiting step during the drug release from the dialysis cassette. Importantly, the final PEG-DSPE concentration in the micelle dispersion inversely affected the release rate of 17-AAG from the micelles. As PEG-DSPE concentration was increased from 0.40 mM to 0.94 mM, the time required for 50% of the drug released from the micelles ($t_{1/2,\ release}$) was prolonged from 2.5 h to 5.8 h. The release of 17-AAG in all formulations appeared to follow the first-order kinetics (Fig. 1B), as suggested by goodness-of-fit being close to unity ($r^2 > 0.99$, Table 1). These results suggest that, by modulating the concentration of the micelle-forming copolymer, PEG-DSPE micelles may serve as drug carriers that retain the encapsulated 17-AAG molecules for an extended period of time.

3.2. In vitro release of 17-AAG from PEG-DSPE/TPGS mixed micelles

In order to further reduce the burst release of 17-AAG from PEG-DSPE micelles, we incorporated TPGS in the composition when preparing the micelles. TPGS is a conjugate of α-tocopherol (vitamin E) and PEG, which has been shown previously to form mixed micelles with PEG-DSPE (Mu et al., 2005; Dabholkar et al., 2006). We hypothesized that the incorporation of TPGS into PEG-DSPE micelles will render a more stable micelle structure, thus decreasing the release rate of 17-AAG from the micelles. We found that, at an equal PEG-DSPE:TPGS molar ratio, TPGS had little effect on the release rate of 17-AAG (data not shown). At a 1:2 molar ratio, PEG-DSPE/TPGS mixed micelles caused over 25% reduction in the release rate compared to their pure PEG-DSPE micelle counterparts (Fig. 1A–D and Table 1). An additional increase of PEG-DSPE:TPGS molar ratio to 1:3 did not further slow the drug release. Therefore, we chose a 1:2 molar ratio of PEG-DSPE:TPGS for the rest of our project. As the concentration of PEG-DSPE was increased from 0.40 mM to 0.94 mM, $t_{1/2,\ release}$ of 17-AAG from the mixed micelles was prolonged from 3.3 h to 7.8 h (Table 1). Neither an increase in the loading concentration of 17-AAG to 6–10 mM nor the presence of 10% fetal calf serum in the micelle dispersion affected the release rate constant of 17-AAG (data not shown). These results indicate that PEG-DSPE/TPGS (at a 1:2 molar ratio) mixed micelles notably improve the retention of 17-AAG compared to pure PEG-DSPE micelles.

3.3. Maximum loading of 17-AAG in PEG-DSPE/TPGS mixed micelles

The maximum loading of 17-AAG into PEG-DSPE/TPGS mixed micelles and pure PEG-DSPE micelles increased almost linearly with PEG-DSPE concentration (Fig. 2). This can be rationalized that, as the concentration of copolymer increases, the number of micelles in the dispersion is increased proportionally. The addition of TPGS into the micelle composition approximately doubled the loading capacity for 17-AAG. PEG-DSPE (12.5 mM)/TPGS (25.0 mM) mixed micelles solubilized about 10.6 mM 17-AAG, yielding an increase of 600-fold in the aqueous solubility of the drug.

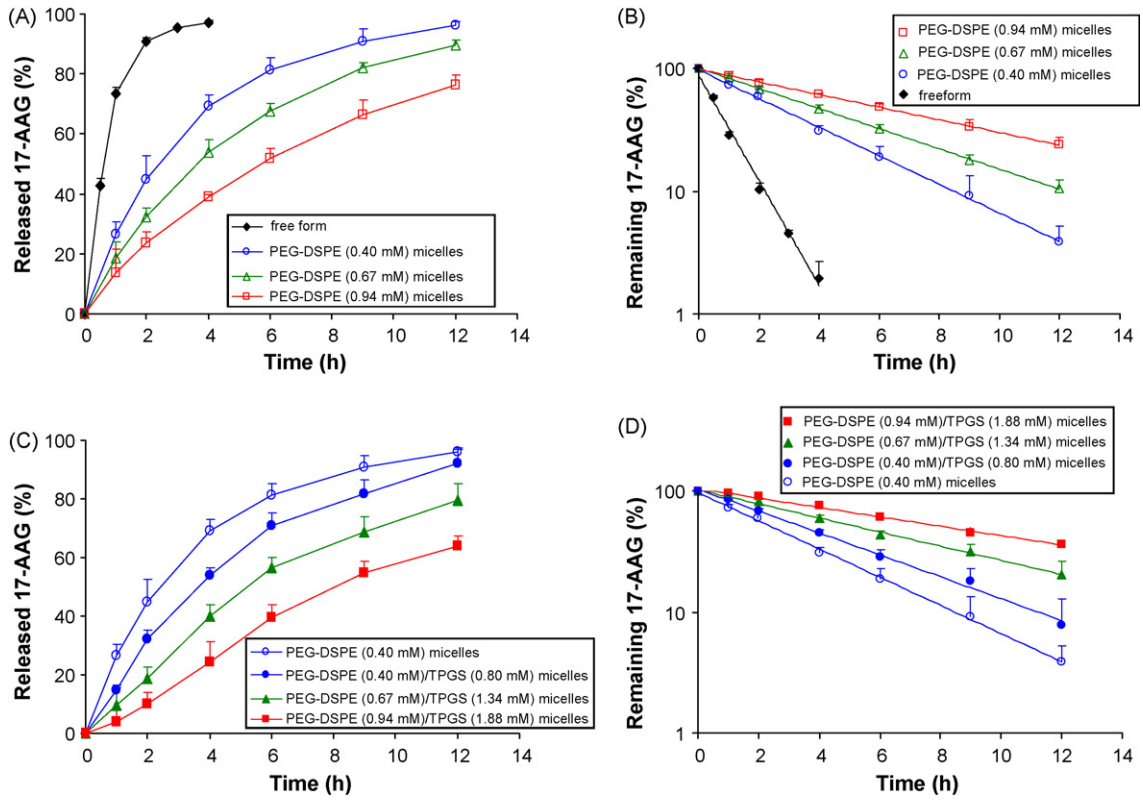

Fig. 1. Release profiles of 17-AAG from micelles under the sink condition. (A) The accumulation of the released 17-AAG from PEG-DSPE micelles as a function of the dialysis time. (B) The retention of the encapsulated 17-AAG by PEG-DSPE micelles as a function of the dialysis time. (C) The accumulation of the released 17-AAG from PEG-DSPE/TPGS mixed micelles as a function of the dialysis time. (D) The retention of the encapsulated 17-AAG by PEG-DSPE/TPGS mixed micelles as a function of the dialysis time. The initial concentration of 17-AAG was kept constant at 45 μM in all samples. Each data point is the mean + SD of three independent experiments. The lines in (B) and (D) represent the respective best-fit nonlinear regression line for each data set.

Table 1
The release parameters of 17-AAG from PEG-DSPE micelles and PEG-DSPE/TPGS mixed micelles as a function of the concentrations of micelle-forming copolymers.

Micelle composition	Release rate constant (h^{-1})	$t_{1/2}$ (h)	Goodness-of-fit (R^2)
Free 17-AAG	0.984	0.7	0.993
PEG-DSPE (0.40 mM) micelles	0.269	2.5	0.998
PEG-DSPE (0.67 mM) micelles	0.189	3.6	0.999
PEG-DSPE (0.94 mM) micelles	0.119	5.8	0.999
PEG-DSPE (0.40 mM)/TPGS (0.80 mM) mixed micelles	0.208	3.3	0.995
PEG-DSPE (0.67 mM)/TPGS (1.34 mM) mixed micelles	0.127	5.4	0.997
PEG-DSPE (0.94 mM)/TPGS (1.88 mM) mixed micelles	0.089	7.8	0.995

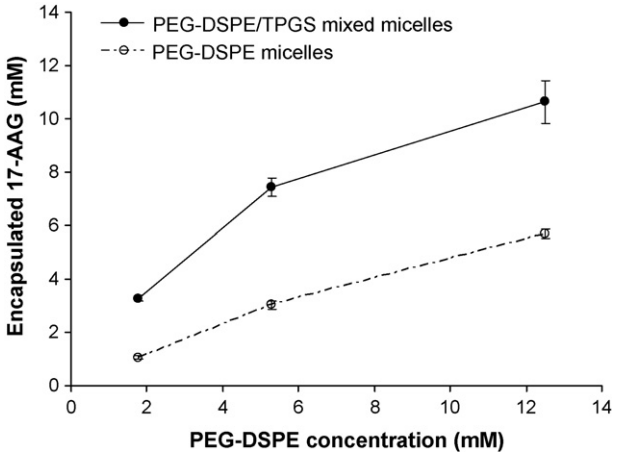

Fig. 2. The maximum loading of 17-AAG as a function of PEG-DSPE concentration in PEG-DSPE micelles and PEG-DSPE/TPGS mixed micelles. Each data point is the mean ± SD of three independent experiments.

3.4. Size measurement of 17-AAG-loaded PEG-DSPE/TPGS micelles

The size distribution of empty PEG-DSPE micelles, empty PEG-DSPE/TPGS mixed micelles and 17-AAG-loaded PEG-DSPE/TPGS mixed micelles are shown in Fig. 3 and Table 2. All micelles exhibited a unimodal and narrow distribution with a size range of 6–25 nm, which were consistent with the sizes of PEG-DSPE-based micelles in the literature (Gao et al., 2002; Lukyanov et al., 2002; Mu et al., 2005; Dabholkar et al., 2006; Musacchio et al., 2009). The inclusion of TPGS (PEG-DSPE:TPGS at a 1:2 molar ratio) in the mixed micelles had no effect on the micelle size, suggesting that TPGS causes little alteration in the aggregation among PEG-DSPE molecules during the micelle formation. The loading of 17-AAG resulted in 1–2 nm upward shift in the size distribution of PEG-DSPE/TPGS mixed micelles, possibly caused by the expansion of the micelle core due to the drug loading. The concentration of PEG-DSPE (0.40–0.94 mM) in the micelle dispersion did not affect the size of micelles, which is indicative that the micelle structure remains constant within the studied concentration range of the copolymer.

Table 2
Representative size distribution of empty and 17-AAG-loaded PEG-DSPE/TPGS mixed micelles.

Micelle composition	Size distribution (%)					
	6.5–7.5 nm	7.5–8.7 nm	8.7–10.1 nm	10.1–11.7 nm	11.7–13.5 nm	13.5–24.4 nm
Empty PEG-DSPE micelles	20.8	24.6	22.8	15.6	8.8	7.4
Empty PEG-DSPE/TPGS mixed micelles	25.1	26.8	22.4	13.9	7.0	4.6
17-AAG-loaded PEG-DSPE/TPGS mixed micelles	3.9	17.0	29.5	26.3	15.0	7.7

3.5. Storage stability of 17-AAG-loaded PEG-DSPE/TPGS mixed micelles

To evaluate the physical stability of the maximally loaded micelles, freshly prepared 17-AAG-incorporating PEG-DSPE/TPGS mixed micelles were incubated at 37 °C or stored at 4 °C, which were evaluated for any changes in their size and drug content. We found that at both temperatures, the particle size of micelles remained constant during the entire period, indicating little structural breakdown or aggregation among micelles. At 37 °C, PEG-DSPE/TPGS micelles retained over 99% of 17-AAG at 24 h. However, at 72 h there was visible drug precipitation and 17-AAG concentration decreased to approximately 40% of the initial concentration. By the end of two weeks, there was only about 12% 17-AAG remaining in the micelle dispersion. In contrast, 17-AAG concentration in the micelle dispersion remained practically unaltered (>99%) at 4 °C throughout the studied duration, indicating that the drug-incorporating micelles are stable and can be stored at 4 °C for at least five weeks without any loss of the drug loading.

3.6. Cytotoxicity of 17-AAG-loaded PEG-DSPE/TPGS mixed micelles

To examine the anticancer effect of 17-AAG-loaded PEG-DSPE/TPGS mixed micelles, we performed the cell proliferation assay. Drug-loaded micelles were prepared using 12.5 mM PEG-DSPE and 25.0 mM TPGS, and the concentration of the incorporated 17-AAG was about 10.6 mM according to the HPLC quantification. As depicted in Fig. 4, 17-AAG-loaded PEG-DSPE/TPGS mixed micelles inhibited the proliferation of human ovarian cancer SKOV-3 cells in a similar manner as free 17-AAG, and there was no statistical difference between these two treatments. As a control, empty PEG-DSPE/TPGS mixed micelles at concentrations equivalent to those present in the drug-loaded micelles caused less than 5% inhibition on the proliferation of SKOV-3 cells. The cytotoxicity of 17-AAG towards SKOV-3 cells observed in this study was consistent with the literature (Sain et al., 2006). These results indicate that 17-AAG-loaded PEG-DSPE/TPGS mixed micelles maintain the cytotoxicity of free 17-AAG.

3.7. ^{1}H NMR analysis of 17-AAG-loaded PEG-DSPE/TPGS mixed micelles

To elucidate the structural features of 17-AAG-loaded micelles and understand the mechanism that responsible for the delayed drug release from PEG-DSPE/TPGS mixed micelles, we carried out a series of ^{1}H NMR experiments. The change in NMR line width can be utilized to examine the formation and dynamics of micelles, and drug encapsulation within micelles. This is because when the internal molecular motion is restricted, nuclear spin–spin relaxation (or T_2 relaxation) is decreased; consequently, the shortened T_2 relaxation broadens the line widths ($\Delta\nu_{1/2}$, FWHH) of NMR signals of the nuclei. The formation of micelles is therefore expected to broaden FWHH of the ^{1}H signals from protons located within the micelle core due to the restricted motion in the hydrophobic region, whereas the rapid motion of the hydrophilic chains in the micelle corona should result in relatively sharper proton signals. We first prepared 17-AAG-incorporating PEG-DSPE micelles with HBS in D_2O. As a control, identical amounts of 17-AAG and PEG-DSPE were mixed and dissolved in DMSO-d_6. The peaks of PEG, DSPE and 17-AAG were assigned by comparing to those of the individual standards in DMSO-d_6 (data not shown). As seen in Fig. 5A, all detected ^{1}H signals of PEG-DSPE and 17-AAG in the DMSO control sample showed narrow line widths, since these protons experience fast molecular motions as expected. Upon the formation of micelles (Fig. 5B), the line width of ^{1}H signal at 3.71 ppm, which originates from oxyethylene ($O–CH_2–CH_2$) protons of PEG, was approximately as narrow as that in DMSO-d_6 ($\Delta\nu_{1/2}$ = 2.81 Hz in D_2O versus 1.83 Hz in DMSO-d_6), indicating that the PEG moiety is located at the corona region of the micelles, where the motion of the protons is not affected significantly by the micelle formation. In contrast, DSPE had much more broadened ^{1}H peaks at 0.87 ppm, 1.28 ppm and ~5–8 ppm in the aqueous micelle sample than the

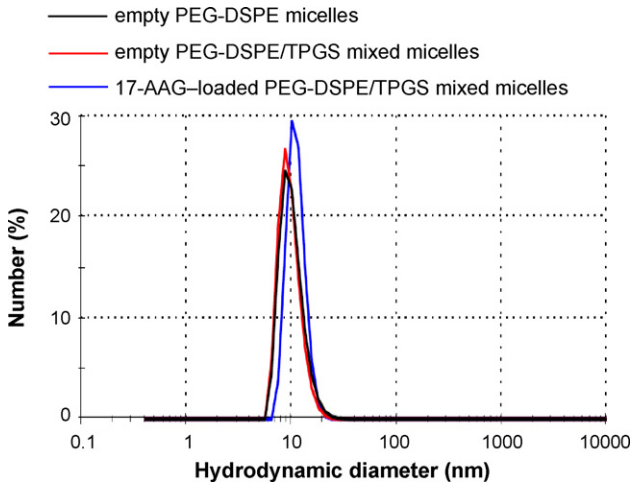

Fig. 3. The size distribution of empty PEG-DSPE micelles, empty PEG-DSPE/TPGS mixed micelles, and 17-AAG-loaded PEG-DSPE/TPGS mixed micelles. Each profile shows representative data obtained from three independent experiments.

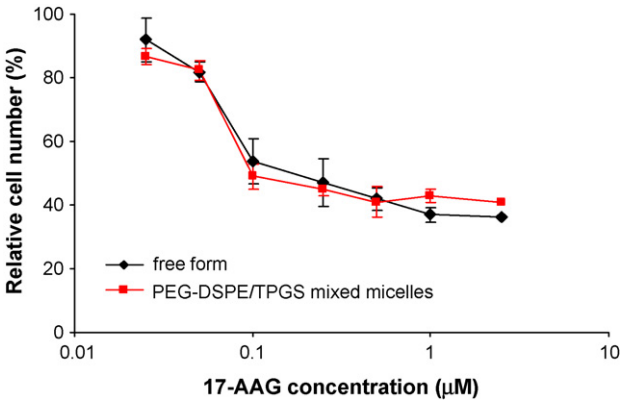

Fig. 4. Cytotoxicity of 17-AAG-loaded PEG-DSPE/TPGS mixed micelles against human ovarian cancer SKOV-3 cells. Results show representative data obtained from three independent experiments and are reported as the means ± SD (n = 3).

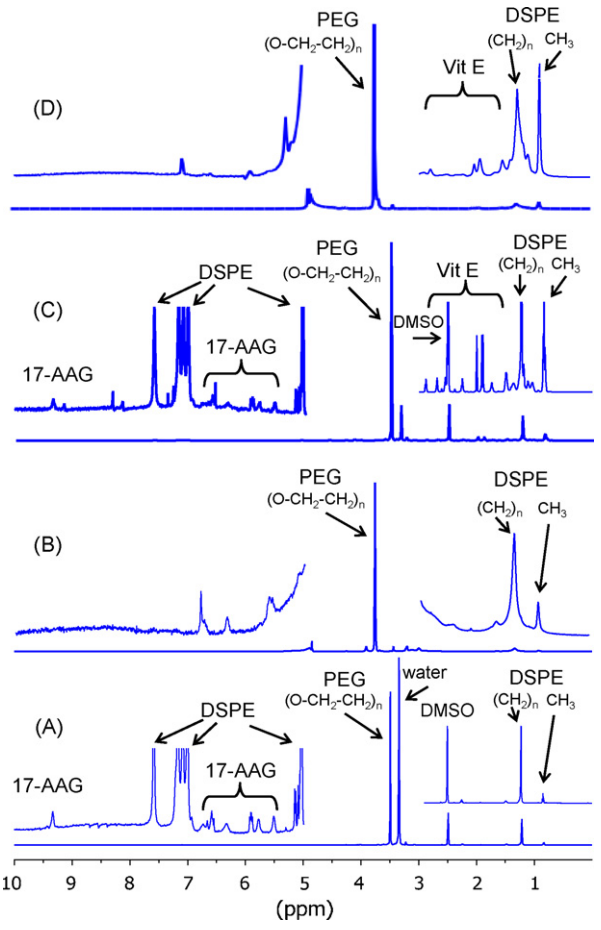

Fig. 5. ^{1}H NMR spectra of (A) the mixture of PEG-DSPE and 17-AAG in DMSO-d_6; (B) 17-AAG-incorporating PEG-DSPE micelles prepared in HBS/D_2O buffer; (C) the mixture of PEG-DSPE, TPGS and 17-AAG in DMSO-d_6; and (D) 17-AAG-incorporating PEG-DSPE/TPGS mixed micelles prepared in HBS/D_2O buffer. The concentrations of PEG-DSPE, TPGS and 17-AAG were 5.3 mM, 10.6 mM and 0.6 mM, respectively. The inserts in the region of 0.0–2.9 ppm and 5.0–10.0 ppm are the intensity-scale expansions. The insert spectra are plotted with different *y*-scales to display the weak peaks. The ^{1}H signals of 17-AAG were not present in the insert of B and D even though the intensity scale was expanded more times than those of A and C. The expanded spectrum at lower frequency region in C is plotted with a *y*-scale larger than that in A in order to display the peaks of the vitamin E moiety in TPGS. As a result, the methylene peak of DSPE at 1.28 ppm was truncated.

DMSO sample. The FWHH of methylene (CH_2) protons of DSPE at 1.28 ppm was increased from 4.95 Hz in DMSO-d_6 (Fig. 5A) to 41.45 Hz in the aqueous micelle sample (Fig. 5B). Moreover, ^{1}H signals of 17-AAG were no longer detectable in the micelle sample. These results clearly demonstrate that the DSPE moiety and 17-AAG in the micelle sample experience much slower motions compared to the DMSO-d_6 control, indicating that they are buried within the hydrophobic core of the micelles.

Next, 17-AAG-incorporating PEG-DSPE/TPGS mixed micelles were studied, and identical amounts of PEG-DSPE, TPGS and 17-AAG dissolved in DMSO-d_6 were used as a control. The proton signals from both copolymers and 17-AAG were observed with sharp line widths in the DMSO-d_6 sample (Fig. 5C). In the aqueous sample, the ^{1}H signals from the vitamin E portion of TPGS were broadened in the micelle sample and those from 17-AAG not detectable (Fig. 5D), indicating that the vitamin E moiety of TPGS and 17-AAG molecules are incorporated into the micelle core. Importantly, the addition of TPGS in the micelle composition further reduced the motion of methylene protons of DSPE as evidenced by the broader peak at 1.28 ppm ($\Delta\nu_{1/2}$ = 57.98 Hz in Fig. 5D) than that of the PEG-DSPE micelles ($\Delta\nu_{1/2}$ = 41.45 Hz in Fig. 5B), suggesting the enhanced hydrophobic interactions within the core of the mixed micelles. Furthermore, compared to the narrow line width in the DMSO control sample, although FWHH of ^{1}H signal of the PEG moiety at 3.71 ppm was slightly increased (from $\Delta\nu_{1/2}$ = 2.85 Hz in Fig. 5C to 3.41 Hz in Fig. 5D), the base of the peak was increased drastically (from 29.15 Hz in Fig. 5C to 95.57 Hz in Fig. 5D). In contrast, the base of the PEG peak in PEG-DSPE micelles was 34.20 Hz (Fig. 5B). As a result of broader line width of the PEG peak in the PEG-DSPE/TPGS mixed micelles, the relative spectral intensity of oxyethylene protons of PEG at 3.71 ppm to methyl (CH_3) protons of DSPE at 0.87 ppm was markedly decreased from 455 in PEG-DSPE micelles (Fig. 5B) to 35 in PEG-DSPE/TPGS mixed micelles (Fig. 5D). These data strongly indicate that the presence of TPGS in the mixed micelles partially limits the mobility of the PEG moiety, resulting in two partitions of PEG protons: one experiencing fast motion and the other with restricted mobility. Taken together, these results provide convincing evidence that the incorporation of TPGS into PEG-DSPE micelles substantially reduces internal molecular motions in both the corona and core regions of the mixed micelles.

4. Discussion

There have been several recent reports on the devise of 17-AAG-loaded polymeric micelles, with the specific intention to eliminate the use of organic solvents and to improve tumor-targeted delivery of the drug. For instance, 17-AAG was incorporated into PEG-poly(D,L-lactide) (PEG-PLA) micelles with a maximum loading of about 2.6–6.6 mM (Shin et al., 2009; Xiong et al., 2009). The release kinetics of 17-AAG-loaded PEG-PLA micelles from the dialysis cassette closely resembled that of free 17-AAG, indicating a very rapid release of 17-AAG molecules from PEG-PLA micelles under the sink condition. Consequently, the drug-loaded PEG-PLA micelles had little impact on the biodisposition of 17-AAG in rats (Xiong et al., 2009). In another recent study, 17-AAG was formulated into vasoactive intestinal peptide-conjugated PEG-DSPE micelles, which exhibited similar cytotoxicity against human breast cancer MCF-7 cells as free 17-AAG. The optimal loading of 17-AAG was determined to be about 0.5 mM in 5 mM PEG-DSPE micelles (Onyüksel et al., 2009). Yet the release of 17-AAG from these micelles was not characterized.

In our current study, PEG-DSPE/TPGS mixed micelles were investigated as nanocarriers for 17-AAG. Compared to pure PEG-DSPE micelles, we found that the addition of TPGS in the micelle composition significantly reduced the release rate constant of 17-AAG. This is most likely because PEG-DSPE/TPGS mixed micelles are thermodynamically more stable than pure PEG-DSPE micelles. Owing to the very low transition temperature (12 °C) of PEG-DSPE molecules, PEG-DSPE micelles are fluid and dynamic complexes that undergo rapid exchange with monomer molecules in the aqueous solution at 37 °C (Kastantin et al., 2009). This thermal motion may destabilize the drug-copolymer association within the micelles, resulting in a fast release of the loaded drug from the micelles. Being approximately half of the molecular size of PEG-DSPE, TPGS molecules are believed to fill the "void" between amphiphilic PEG-DSPE chains, as they spontaneously orient and form spheroidal "core–shell" micelle structure (Fig. 6). As supported by our ^{1}H NMR results, the insertion of TPGS into PEG-DSPE micelles strengthened the hydrophobic interactions within the micelle core, as well as partially restricted dynamic motion of PEG chains in the corona region, which may collectively elevate the activation energy required for monomer desorption and thus decrease monomer exchange kinetics of the micelles.

Furthermore, the incorporation of TPGS in the micelle composition strikingly enhanced the encapsulation capacity for 17-AAG. This is believed to be a result of increased hydrophobic interac-

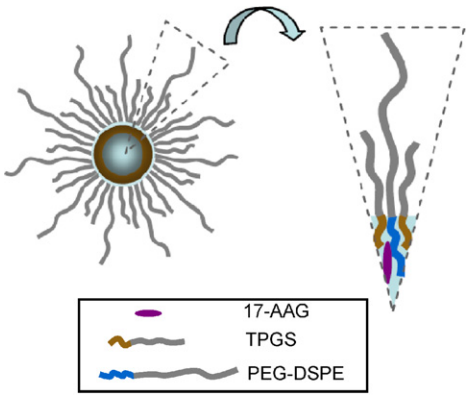

Fig. 6. The proposed structure scheme of 17-AAG-loaded PEG-DSPE/TPGS mixed micelle.

tions in the micelle core, which drive the micellar solubilization of lipophilic molecules. In particular, PEG-DSPE (12.5 mM)/TPGS (25.0 mM) mixed micelles had a maximum loading capacity of about 10.6 mM for 17-AAG, which makes these drug carriers well suited for delivering clinically relevant concentration of 17-AAG to the tumor cells *in vivo*. Similarly improved drug loading into PEG-DSPE/TPGS mixed micelles has been previously observed for other water-insoluble drugs such as camptothecin and paclitaxel (Mu et al., 2005; Dabholkar et al., 2006).

One crucial finding of our study is that the release rate constant of 17-AAG from PEG-DSPE/TPGS mixed micelles was inversely affected by the final concentration of PEG-DSPE, even though the studied concentration range was well above the CMC of the copolymer and the hydrodynamic diameter of these micelles remained constant. To our knowledge, this is the first time that copolymer concentration-dependent drug release from micelles has been reported. While the molecular mechanism responsible for such phenomenon remains to be elucidated, a plausible explanation to consider is that, being fluid and dynamic complexes, PEG-DSPE micelles are likely to cause fast oscillation of 17-AAG molecules between the micelle core and the aqueous solution, a delicate balance determined by the physicochemical properties of 17-AAG. Since an increased copolymer concentration gives rise to more micelle entities, the probability of 17-AAG molecules returning into micelles may therefore increase, leading to an apparent decline in the release rate constant. This finding has important implication when devising PEG-DSPE micellar nanocarriers for tumor-targeted delivery of 17-AAG *in vivo*. It suggests that the plasma concentration of PEG-DSPE needs to substantially exceed its CMC, in order to minimize premature drug release from micellar carriers to the systemic circulation.

Compared to the extremely slow release of some chemotherapeutic agents (Mu et al., 2005; Dabholkar et al., 2006), the release of 17-AAG from PEG-DSPE/TPGS mixed micelles appears to be relatively fast. This may be rationalized by the compatibility between the incorporated drug and the micelle core, which is determined by the physicochemical properties intrinsic to the drug molecules. When administered *in vivo*, albeit some loaded 17-AAG molecules will inevitably be prematurely released from these micellar carriers, it is conceivable that a significant proportion of 17-AAG-loaded PEG-DSPE/TPGS micelles may still be able to preferentially accumulate at the tumor site via the EPR effect, improving the pharmacokinetic characteristics of free 17-AAG. This is because the extravasation of PEG-DSPE micelles to the tumor tissue occurs rapidly following intravenous administration and reaches a plateau by 4–5 h. The prolongation of the release half-life of 17-AAG from micelles beyond this time frame will therefore be of critical consequence in extending the circulation time of the drug-incorporating micelles and achieving targeted drug delivery to the tumor tissue.

In summary, we have demonstrated the feasibility of utilizing PEG-DSPE/TPGS mixed micelles as novel nanocarriers for 17-AAG. The incorporation of TPGS in the micelle composition restricted molecular motions of copolymers in both the corona and core regions the micelles, significantly delaying the release of 17-AAG. By optimizing the concentrations of micelle-forming copolymers, therapeutically relevant concentration of 17-AAG could be dispensed in PEG-DSPE/TPGS mixed micelles without the inclusion of any organic solvents. PEG-DSPE/TPGS mixed micelles offer a promising platform for facile generation of multifunctional nanocarriers for delivering 17-AAG to tumor cells via active targeting.

Acknowledgements

This work was supported by the New Investigators Program of the American Association of College of Pharmacy (C.T.). This work has been subjected to review by the National Exposure Research Laboratory and approved for publication. Approval does not signify that the contents reflect the views of the Agency, nor does its mention of trade names or commercial products constitute endorsement or recommendation for use.

References

Dabholkar, R.D., Sawant, R.M., Mongayt, D.A., Devarajan, P.V., Torchilin, V.P., 2006. Polyethylene glycol–phosphatidylethanolamine conjugate (PEG–PE)-based mixed micelles: some properties, loading with paclitaxel, and modulation of P-glycoprotein-mediated efflux. Int. J. Pharm. 315, 148–157.

Egorin, M.J., Zuhowski, E.G., Rosen, D.M., Sentz, D.L., Covey, J.M., Eiseman, J.J., 2001. Plasma pharmacokinetics and tissue distribution of 17-(allylamino)-17-demethoxygeldanamycin (NSC 330507) in CD2F1 mice. Cancer Chemother. Pharmacol. 47, 291–302.

Egorin, M.J., Lagattuta, T.F., Hamburger, D.R., Covey, J.M., White, K.D., Musser, S.M., Eiseman, J.L., 2002. Pharmacokinetics, tissue distribution, and metabolism of 17-(dimethylaminoethylamino)-17-demethoxygeldanamycin (NSC 707545) in CD2F1 mice and Fischer 344 rats. Cancer Chemother. Pharmacol. 49, 7–19.

Erlichman, C., 2009. Tanespimycin: the opportunities and challenges of targeting heat shock protein 90. Expert Opin. Investig. Drugs 18, 861–868.

Gao, Z., Lukyanov, A.N., Singhal, A., Torchilin, V.P., 2002. Diacyllipid-polymer micelles as nanocarriers for poorly soluble anticancer drugs. Nano Lett. 2, 979–982.

Gaucher, G., Dufresne, M.-H., Sant, V.P., Kang, N., Maysinger, D., Leroux, J.-C., 2005. Block copolymer micelles: preparation, characterization and application in drug delivery. J. Control. Release 109, 169–188.

Glaze, E.R., Lambert, A.L., Smith, A.C., Page, J.G., Johnson, W.D., McCormick, D.L., Brown, A.P., Levine, B.S., Covey, J.M., Egorin, M.J., Eiseman, J.L., Holleran, J.L., Sausville, E.A., Tomaszewski, J.E., 2005. Preclinical toxicity of a geldanamycin analog, 17-(dimethylaminoethylamino)-17-demethoxygeldanamycin (17-DMAG), in rats and dogs: potential clinical relevance. Cancer Chemother. Pharmacol. 56, 637–647.

Goetz, M.P., Toft, D., Reid, J., Ames, M., Stensgard, B., Safgren, S., Adjei, A.A., Sloan, J., Atherton, P., Vasile, V., Salazaar, S., Adjei, A., Croghan, G., Erlichman, C., 2005. Phase I trial of 17-allylamino-17-demethoxygeldanamycin in patients with advanced cancer. J. Clin. Oncol. 23, 1078–1087.

Grem, J.L., Morrison, G., Guo, X.-D., Agnew, E., Takimoto, C.H., Thomas, R., Szabo, E., Grochow, L., Grollman, F., Hamilton, J.M., Neckers, L., Wilson, R.H., 2005. Phase I and pharmacologic study of 17-(allylamino)-17-demethoxygeldanamycin in adult patients with solid tumors. J. Clin. Oncol. 23, 1885–1893.

Guo, W., Reigan, P., Siegel, D., Ross, D., 2008. Enzymatic reduction and glutathione conjugation of benzoquinone ansamycin heat shock protein 90 inhibitors: relevance for toxicity and mechanism of action. Drug Metab. Dispos. 36, 2050–2057.

Heath, E.I., Hilman, D.W., Vaishampayan, U., Sheng, S., Sarkar, F., Harperet, F., Gaskins, M., Pitot, H.C., Tan, W., Ivy, S.P., Pili, R., Carducci, M.A., Erlichman, C., Liu, G., 2008. A phase II trial of 17-allylamino-17-demethoxygeldanamycin in patients with hormone-refractory metastatic prostate cancer. Clin. Cancer Res. 14, 7940–7946.

Hollingshead, M., Alley, M., Burger, A.M., Borgel, S., Pacula-Cox, C., Fiebig, H.-H., Sausville, E.A., 2005. *In vivo* antitumor efficacy of 17-DMAG (17-dimethylaminoethylamino-17-demethoxygeldanamycin hydrochloride), a water-soluble geldanamycin derivative. Cancer Chemother. Pharmacol. 56, 115–125.

Isaacs, J.S., Xu, W., Neckers, L., 2003. Heat shock protein 90 as a molecular target for cancer therapeutics. Cancer Cell 3, 213–217.

Kastantin, M., Ananthanarayanan, B., Karmali, P., Ruoslahti, E., Tirrell, M., 2009. Effect of the lipid chain melting transition on the stability of DSPE-PEG(2000) micelles. Langmuir 25, 7279–7286.

Lukyanov, A.N., Gao, Z., Mazzola, L., Torchilin, V.P., 2002. Polyethylene glycol–diacyllipid micelles demonstrate increased accumulation insubcutaneous tumors in mice. Pharm. Res. 19, 1424–1429.

Matsumura, Y., Maeda, H., 1986. A new concept for macromolecular therapeutics in cancer chemotherapy: mechanism of tumoritropic accumulation of proteins and the antitumor agent Smancs. Cancer Res. 46, 6387–6392.

Matsumura, Y., 2008. Poly(amino acid) micelles nanocarriers in preclinical and clinical studies. Adv. Drug Deliv. Rev. 60, 899–914.

Modi, S., Stopeck, A.T., Gordon, M.S., Mendelson, D., Solit, D.B., Bagatell, R., Ma, W., Wheler, J., Rosen, N., Norton, L., Cropp, G.F., Johnson, R.G., Hannah, A.L., Hudis, C.A., 2007. Combination of trastuzumab and tanespimycin (17-AAG, KOS-953) is safe and active in trastuzumab-refractory HER-2-overexpressing breast cancer: a phase I dose-escalation study. J. Clin. Oncol. 25, 5410–5417.

Mu, L., Elbayoumi, T.A., Torchilin, V.P., 2005. Mixed micelles made of poly(ethylene glycol)-phosphatidylethanolamine conjugate and D-α-tocopheryl polyethylene glycol 1000 succinate as pharmaceutical nanocarriers for camptothecin. Int. J. Pharm. 306, 142–149.

Musacchio, T., Laquintana, V., Latrofa, A., Trapani, G., Torchilin, V.P., 2009. PEG–PE micelles loaded with paclitaxel and surface-modified by a PBR-ligand: synergistic anticancer effect. Mol. Pharm. 6, 468–479.

Nishiyama, N., Kataoka, K., 2006. Current state, achievements, and future prospects of polymeric micelles as nanocarriers for drug and gene delivery. Pharmacol. Ther. 112, 630–648.

Onyüksel, H., Mohanty, P.S., Rubinstein, I., 2009. VIP-grafted sterically stabilized phospholipid nanomicellar 17-allylamino-17-demethoxy geldanamycin: a novel targeted nanomedicine for breast cancer. Int. J. Pharm. 365, 157–161.

Ramalingan, S.S., Egorin, M.J., Ramanathan, R.K., Remick, S.C., Sikorski, R.P., Lagattuta, T.F., Chatta, G.S., Friedland, D.M., Stoller, R.G., Potter, D.M., Ivy, S.P., Belani, C.P., 2008. A phase I study of 17-allyamino-17-demethoxygeldanamycin combined with paclitaxel in patients with advanced solid malignancies. Clin. Cancer Res. 14, 3456–3461.

Roforth, M.M., Tan, C., 2008. Combination of rapamycin and 17-allylamino-17-demethoxygeldanamycin abrogates Akt activation and potentiates mTOR blockade in breast cancer cells. Anti-Cancer Drugs 19, 681–688.

Sain, N., Krishnan, B., Ormerod, M.G., Rienzo, A.D., Liu, W.M., Kaye, S.B., Workman, P., Jackman, A.L., 2006. Potentiation of paclitaxel activity by the HSP90 inhibitor 17-allylamino-17-demthoxygeldanamycin in human ovarian carcinoma cell lines with high levels of activated AKT. Mol. Cancer Ther. 5, 1197–1208.

Shin, H.-C., Alani, A.W.G., Rao, D.A., Rockich, N.C., Kwon, G.S., 2009. Multi-drug loaded polymeric micelles for simultaneous delivery of poorly soluble anticancer drug. J. Control. Release 14, 294–300.

Solit, D.B., Ivy, S.P., Kopil, C., Sikorski, R., Morris, M.J., Slovin, S.F., Kelly, W.K., DeLaCruz, A., Curley, T., Heller, G., Larson, S., Schwartz, L., Egorin, M.J., Rosen, N., Scher, H.I., 2007. Phase I trial of 17-allyamino-17-demethoxygeldanamycin in patients with advanced cancer. Clin. Cancer Res. 13, 1775–1782.

Solit, D.S., Osman, I., Polsky, D., Panageas, K.S., Daud, A., Goydos, J.S., Teitcher, J., Wolchok, J.D., Germino, F.J., Krown, S.E., Coit, D., Rosen, N., Chapman, P.B., 2008. Phase II trial of 17-allylamino-17-demethoxygeldanamycin in patients with metastatic melanoma. Clin. Cancer Res. 14, 8302–8307.

Sydor, J.R., Normant, E., Pien, C.S., Porter, J.R., Ge, J., Grenier, L., Pak, R.H., Ali, J.A., Dembski, M.S., Hudak, J., Patterson, J., Penders, C., Pink, M., Read, M.A., Sang, J., Woodward, C., Zhang, Y., Grayzel, D.S., Wright, J., Barrett, J.A., Palombella, V.J., Adams, J., Tong, J.K., 2006. Development of 17-allylamino-17-demethoxygeldanamycin hydroquinone hydrochloride (IPI-504), an anti-cancer agent directed against Hsp90. Proc. Natl. Acad. Sci. U.S.A. 103, 17408–17413.

Tang, N., Du, G., Wang, N., Liu, C., Hang, H., Liang, W., 2007. Improving penetration in tumors with nanoassemblies of phospholipids and doxorubicin. J. Natl. Cancer Inst. 99, 1004–1015.

Tse, A.N., Klimstra, D.S., Gonen, M., Shah, M., Sheikh, T., Sikorski, R., Carvajal, R., Mui, J., Tipian, C., O'Reilly, E., Chung, K., Maki, R., Lefkowitz, R., Brown, K., Manova-Todorova, K., Wu, N., Egorin, M.J., Kelsen, D., Schwartz, G.K., 2008. A phase I dose-escalation study of irinotecan in combination with 17-allyamino-17-demethoxygeldanamycin in patients with solid tumors. Clin. Cancer Res. 14, 6704–6711.

Weigel, B.J., Blaney, S.M., Reid, J.M., Safgren, S.L., Bagatell, R., Kersey, J., Neglia, J.P., Ivy, S.P., Ingle, A.M., Whitesell, L., Gilbertson, R.J., Krailo, M., Ames, M., Adamson, P.C., 2007. A phase I study of 17-allyaminogeldanamycin in relapsed/refractory pediatric patients with solid tumors: a children oncology group study. Clin. Cancer Res. 13, 1789–1793.

Whitesell, L., Lindquist, S.L., 2005. HSP90 and the chaperoning of cancer. Nat. Rev. Cancer 5, 761–772.

Xiong, M.P., Yáñez, J.A., Kwon, G.S., Davies, N.M., Forrest, M.L., 2009. A cremophor-free formulation for tanespimycin (17-AAG) using PEO-b-PDLLA micelles: characterization and pharmacokinetics in rats. J. Pharm. Sci. 98, 1577–1586.